Andreev reflection through a quantum dot coupled with two ferromagnets and a superconductor

Yu Zhu, Qing-feng Sun, and Tsung-han Lin*
State Key Laboratory for Mesoscopic Physics and Department of Physics, Peking University, Beijing 100871, China
(Received 6 April 2001; published 19 December 2001)

We study the Andreev reflection (AR) in a three-terminal mesoscopic hybrid system, in which two ferromagnets (F_1 and F_2) are coupled to a superconductor (S) through a quantum dot. By using nonequilibrium Green function, we derive a general current formula which allows arbitrary spin polarizations, magnetization orientations, and bias voltages in F_1 and F_2. The formula is applied to study both zero bias conductance and finite bias current. The current conducted by crossed AR involving F_1, F_2, and S is particularly unusual, in which an electron with spin σ incident from one of the ferromagnets picks up another electron with spin $\bar{\sigma}$ from the other one, both enter S and form a Cooper pair. Several special cases are investigated to reveal the properties of AR in this system.

DOI: 10.1103/PhysRevB.65.024516 PACS number(s): 74.50.+r, 73.40.Gk, 75.70.Pa

I. INTRODUCTION

Electrons have spin as well as charge. The application of the electron-spin property opens a fruitful field in the transport of ferromagnetic materials, such as the discovery of giant magnetoresistance (GMR) and tunnel magnetoresistance (TMR) effects.[1] On the other hand, there is growing interest in the mesoscopic normal-metal/superconductor (N/S) hybrid system,[2] in which Andreev reflection (AR) at the N/S interface plays an important role in the low bias voltage regime.[3] In the AR process, an electron incident with energy E and spin σ picks up another electron with energy $-E$ and spin $\bar{\sigma}$, both enter S and form a Cooper pair, leaving an Andreev reflected hole in the N side. One may expect that the interplay of the spin property of the AR process and the spin-dependent transport in ferromagnetic materials will add new physics to mesoscopic hybrid systems, and to the future applications of spintronics.

Several works have been devoted to this issue. In the pioneering work of de Jong *et al.*,[4] the transport of a ferromagnet/superconductor (F/S) junction was studied by scattering matrix formalism. The conductance of AR is shown to be strongly affected by the spin polarization of F. The idea was verified by recent experiments in F/S thin-film nanocontact[5] and F/S metallic point contact.[6] Especially, in Ref. 6, Soulen *et al.* successfully determined the spin polarization at the Fermi energy for several metals by measuring the differential conductance of F/S metallic point contact. Further calculations[7] implied that the Fermi velocity mismatch between F and S also affects the AR conductance of F/S contact, and the conductance may even be enhanced in the presence of spin polarization. In addition to simple F/S junction, F/S contact with S in d-wave symmetry,[7,8] F/S nanostructure with giant proximity effect,[9,10] and more complicated structures such as FSF double junctions,[11–13] SFS double junctions,[14–16] S/F superlattices,[17] and $(NF)_nS$ multilayer structures[18,19] were also investigated.

In this paper, we propose an idea that two sources of spin polarized electrons with different orientations are injected into a superconductor, which can be achieved by a three terminal mesoscopic F/S hybrid structure shown in Fig. 1. In this system, a central quantum dot (QD) is coupled via tunnel barriers to two ferromagnetic electrodes (F_1 and F_2) and a superconducting electrode (S) [hereafter, the system is simply referred as to (F_1,F_2)-QD-S]. F_1 and F_2 are assumed to have arbitrary magnetization orientations, spin polarizations, and bias voltages. The bias voltage of S is set to zero as the ground. QD is designed to provide a link between F_1, F_2, and S, so that AR can take place through discrete energy states of QD. Consider the special case that F_1 and F_2 are fully polarized, AR only involving F_1 and S or only involving F_2 and S are completely suppressed, while the crossed AR involving F_1, F_2, and S depends strongly on the magnetization orientations of F_1 and F_2, being suppressed if they are in ferromagnetic alignment, enhanced in antiferromagnetic alignment. In this paper, we will derive a current formula by using the nonequilibrium Green-function method, and investigate several special cases to illustrate the properties of AR's in this system.

During the preparation of this paper, we became aware that in the recent publication of Deutscher *et al.*[20] a device consisting of two point contacts between two ferromagnetic tips and a superconductor was proposed. For the two tips with fully but opposite spin polarizations, they suggested that ''mixed'' Cooper pair made of electrons coming one from each tip can be injected into the superconductor, leading to unusual properties of such a device. Section IV of this paper is partially stimulated by their work.

The rest of this paper is organized as follows: In Sec. II, we present the model Hamiltonian and a general current formula for the hybrid system (F_1,F_2)-QD-S by nonequilibrium Green-function method. In Sec. III, we study the zero-

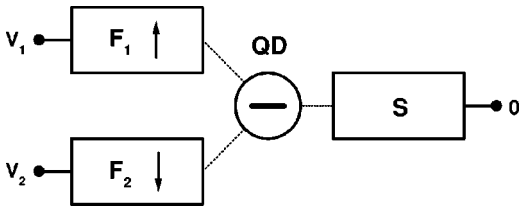

FIG. 1. Schematic drawing of the three-terminal system under consideration. F_1 and F_2 represent two ferromagnetic electrodes with different magnetization orientations and bias voltages, QD is a quantum dot, and S is a superconductor with zero voltage as the ground.

bias conductance, assuming $V_1=V_2=0^+$. The explicit forms of the conductance are presented and numerically studied. In Sec. IV, we study the finite bias current with F_1 and F_2 in antiferromagnetic alignment, and the fully spin polarized case is discussed in detail. Finally, a brief summary is given in Sec. V.

II. MODEL AND FORMULATION

The system under consideration can be described by the following Hamiltonian:

$$H=H_1+H_2+H_{dot}+H_s+H_T, \tag{1}$$

$$H_1=\sum_{k\sigma}(\epsilon_k-\sigma h_1-\mu_1)a^\dagger_{k\sigma}a_{k\sigma},$$

$$H_2=\sum_{k\sigma'}(\epsilon_k-\sigma' h_2-\mu_2)b^\dagger_{k\sigma'}b_{k\sigma'},$$

$$H_{dot}=E_0\sum_\sigma c^\dagger_\sigma c_\sigma,$$

$$H_s=\sum_{p\sigma}\epsilon_p d^\dagger_{p\sigma}d_{p\sigma}+\sum_p[\Delta d^\dagger_{p\uparrow}d^\dagger_{-p\downarrow}+\text{H.c.}],$$

$$H_T=\sum_{k\sigma}[t_{1\sigma}a^\dagger_{k\sigma}c_\sigma+\text{H.c.}]+\sum_{k\sigma}[t_{2\sigma}b^\dagger_{k\sigma}c_\sigma+\text{H.c.}]+\sum_{p\sigma}[t_s d^\dagger_{p\sigma}c_\sigma+\text{H.c.}].$$

H_1 and H_2 are the Hamiltonians of F_1 and F_2 in the mean-field approximation, with different magnetization orientations and chemical potentials. The spin bands of $F_1(F_2)$ are split by $2h_1(2h_2)$ due to the exchange energy. The magnetization orientation of F_1 is set as the z axis, while the orientation of F_2 as the z' axis which has an angle θ with respect to the z axis. The operators with the spin-quantization axis z and the operators with the spin-quantization axis z' are related by the $D^{1/2}$ matrix as

$$\begin{pmatrix} b^\dagger_{k\uparrow'} \\ b^\dagger_{k\downarrow'} \end{pmatrix}=\begin{pmatrix} \cos\frac{\theta}{2} & -\sin\frac{\theta}{2} \\ \sin\frac{\theta}{2} & \cos\frac{\theta}{2} \end{pmatrix}\begin{pmatrix} b^\dagger_{k\uparrow} \\ b^\dagger_{k\downarrow} \end{pmatrix}. \tag{2}$$

H_{dot} describes the quantum dot, in which only one spin degenerate level is considered and the intradot interaction is ignored for simplicity. H_s is the Hamiltonian for a BCS superconductor with the chemical potential fixed to zero as the ground. H_T depicts the tunneling between QD and F_1, F_2, and S, coupling different parts of the system together.

By introducing a 4×4 matrix representation and using the nonequilibrium Green-function technique (see the Appendix for details), we derive the formula of the current flowing from F_1 to the QD as

$$I_1=\frac{e}{h}\int d\omega[A_{11}(f_1-\bar{f}_1)+A_{12}(f_1-\bar{f}_2)+Q_{1s}(f_1-f_s)+Q_{12}(f_1-f_2)], \tag{3}$$

in which

$$A_{11}=\Gamma_{1\uparrow}(\Gamma_{1\downarrow}|G^r_{12}|^2+\Gamma_{1\uparrow}|G^r_{14}|^2)+\Gamma_{1\downarrow}(\Gamma_{1\uparrow}|G^r_{34}|^2+\Gamma_{1\downarrow}|G^r_{32}|^2), \tag{4}$$

$$A_{12}=\Gamma_{1\uparrow}[(c^2\Gamma_{2\downarrow}+s^2\Gamma_{2\uparrow})|G^r_{12}|^2+(c^2\Gamma_{2\uparrow}+s^2\Gamma_{2\downarrow})|G^r_{14}|^2]+\Gamma_{1\downarrow}[(c^2\Gamma_{2\uparrow}+s^2\Gamma_{2\downarrow})|G^r_{34}|^2+(c^2\Gamma_{2\downarrow}+s^2\Gamma_{2\uparrow})|G^r_{32}|^2]+sc(\Gamma_{2\uparrow}-\Gamma_{2\downarrow})2\,\text{Re}(\Gamma_{1\uparrow}G^r_{12}G^{r*}_{14}+\Gamma_{1\downarrow}G^r_{32}G^{r*}_{34}), \tag{5}$$

$$Q_{1s}=\Gamma_{1\uparrow}\Gamma_s\tilde{\rho}\left[|G^r_{11}|^2+|G^r_{12}|^2+|G^r_{13}|^2+|G^r_{14}|^2+2\,\text{Re}\left(-\frac{\Delta}{\omega}G^r_{11}G^{r*}_{12}+\frac{\Delta}{\omega}G^r_{13}G^{r*}_{14}\right)\right]+\Gamma_{1\downarrow}\Gamma_s\tilde{\rho}\left[|G^r_{31}|^2+|G^r_{32}|^2+|G^r_{33}|^2+|G^r_{34}|^2+2\,\text{Re}\left(-\frac{\Delta}{\omega}G^r_{31}G^{r*}_{32}+\frac{\Delta}{\omega}G^r_{33}G^{r*}_{34}\right)\right], \tag{6}$$

$$Q_{12}=\Gamma_{1\uparrow}[(c^2\Gamma_{2\uparrow}+s^2\Gamma_{2\downarrow})|G^r_{11}|^2+(c^2\Gamma_{2\downarrow}+s^2\Gamma_{2\uparrow})|G^r_{13}|^2]+\Gamma_{1\downarrow}[(c^2\Gamma_{2\downarrow}+s^2\Gamma_{2\uparrow})|G^r_{33}|^2+(c^2\Gamma_{2\uparrow}+s^2\Gamma_{2\downarrow})|G^r_{31}|^2]+sc(\Gamma_{2\uparrow}-\Gamma_{2\downarrow})2\,\text{Re}(\Gamma_{1\uparrow}G^r_{11}G^{r*}_{13}+\Gamma_{1\downarrow}G^r_{33}G^{r*}_{31}), \tag{7}$$

with $\tilde{\rho}(\omega)\equiv(|\omega|/\sqrt{\omega^2-\Delta^2})\theta(|\omega|-\Delta)$ being the ordinary BCS density of states, s and c for the short notations of $\sin\theta/2$ and $\cos\theta/2$. f_1, $\bar{f}_1$, f_2, $\bar{f}_2$, and f denote $f(\omega-V_1)$, $f(\omega+V_1)$, $f(\omega-V_2)$, $f(\omega+V_2)$, and $f(\omega)$, respectively, where $f(\omega)$ is the Fermi distribution function.

The current formula is composed of four contributions from different conducting processes: (i) $A_{11}(f_1-\bar{f}_1)$ represents the Andreev reflection through F_1-QD-S, i.e., an electron of F_1 is reflected by S into a hole of F_1, which can be judged by the thermal factor $(f_1-\bar{f}_1)$. The probability A_{11} has four terms, in which $\Gamma_{1\uparrow}\Gamma_{1\downarrow}|G^r_{12}|^2$ is for the subprocess that an electron with spin↑ is Andreev reflected into a hole with spin↓; $\Gamma_{1\uparrow}\Gamma_{1\uparrow}|G^r_{14}|^2$ is for an electron with spin↑ first flips its spin in QD due to F_2, then Andreev reflected into a hole with spin↑; while the other two terms are for the similar subprocesses involving the electron incident with spin↓ [see Eq. (A2) for the physical meaning of the elements of **G**]. (ii) $A_{12}(f_1-\bar{f}_2)$ represents the crossed Andreev reflection through (F_1,F_2)-QD-S, i.e., an electron of F_1 is reflected by S into a hole of F_2, judged by the thermal factor $(f_1-\bar{f}_2)$. The probability A_{12} is much more complicated than A_{11}, since the polarization orientation of F_2 has an angle θ to the chosen spin-quantization axis. The first four terms can be

interpreted similarly to those of A_{11}, by "projecting" the spin polarization of F_2 to the chosen axis, while the last four can be viewed as their interference terms. (iii) $Q_{1s}(f_1-f_s)$ represents the single-particle tunneling through F_1-QD-S, judged by the thermal factor (f_1-f_s). The probability Q_{1s} can be divided into two subgroups, corresponding to the processes involving electron with spin↑ and spin↓, respectively. Each subgroup contains four subprocesses and their interference terms. (iv) $Q_{12}(f_1-f_2)$ represents the single-particle tunneling through F_1-QD-F_2, and the probability Q_{12} can be analyzed similarly to the above three. (A similar physical interpretation can be found in Refs. 21 and 22.)

One can obtain the current flowing from F_2 simply by exchanging the indices 1 and 2 in the above formula, and the current flowing from S can be deduced by the relation of the current conservation, $I_1+I_2+I_s=0$. The current formulas Eqs. (3)–(7) are the central result of this work, which can be applied to ferromagnetic electrodes F_1 and F_2 with arbitrary spin polarizations, magnetization orientations, and bias voltages.

In the following numerical studies, we assume that $|eV_1|$, $|eV_2|<\Delta$, and $k_BT\ll\Delta$. The Q_{1s} process will vanish because of the factor $\tilde{\rho}$ and the Fermi function difference (f_1-f_s). The Q_{12} process will be ruled out in two special cases: F_1 and F_2 are either equally biased (Sec. III) or fully but oppositely polarized (Sec. IV). We will concentrate on AR processes A_{11} (direct AR through F_1-QD-S) and A_{12} [crossed AR through (F_1,F_2)-QD-S], and investigate several special cases to illustrate the properties of these two AR's.

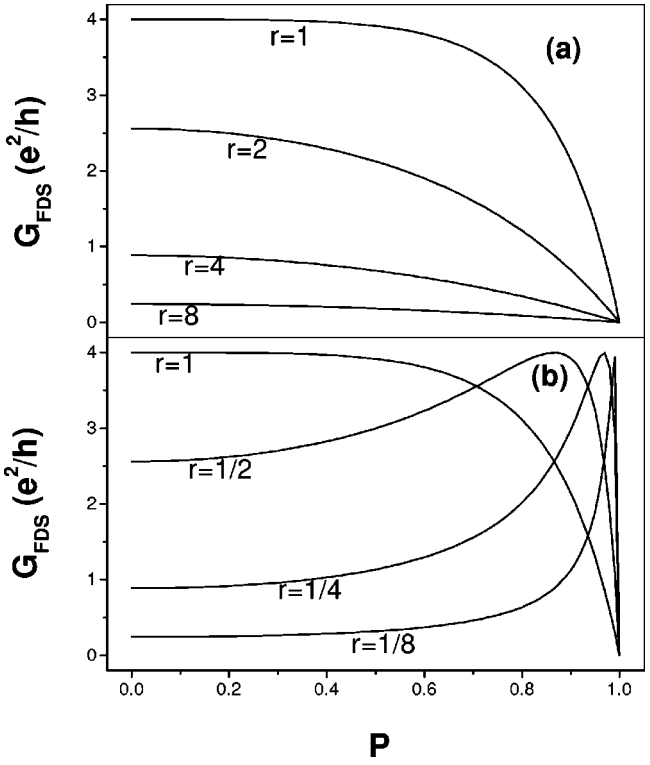

FIG. 2. The zero-bias conductance G vs P for F-QD-S, where P is the spin polarization of F. $r\equiv\Gamma_R/\Gamma_L$ is the ratio of coupling strengths, with $r\geqslant 1$ for (a) and $r\leqslant 1$ for (b).

III. ZERO-BIAS CONDUCTANCE

In this section, we study the zero-bias conductance by taking $V_1=V_2=0^+$. Since there is no bias voltage between F_1 and F_2, there is no net single-particle current flowing between them. For $k_BT\ll\Delta$, the single-particle current from F_1 or F_2 to S is also negligible. Therefore only AR's contribute to the conductance. For simplicity, we set $k_BT=0$ and $E_0=0$, introduce the spin polarization $P_\beta\equiv(\Gamma_{\beta\uparrow}-\Gamma_{\beta\downarrow})/(\Gamma_{\beta\uparrow}+\Gamma_{\beta\downarrow})$, and the spin-averaged coupling strength $\Gamma_\beta\equiv\frac{1}{2}(\Gamma_{\beta\uparrow}+\Gamma_{\beta\downarrow})$, with $\beta=1,2$ for F_1 and F_2, respectively.

First consider the simplest case in which $\Gamma_2=0$, $\Gamma_1\equiv\Gamma_L, P_1\equiv P, \Gamma_s\equiv\Gamma_R$. Then the three-terminal system (F_1,F_2)-QD-S reduces to a two-terminal system F-QD-S, and the conductance is easily obtained from the current formula as

$$G_{FDS}=\frac{4e^2}{h}\frac{(1-P^2)r^2}{(1-P^2+r^2)^2}, \tag{8}$$

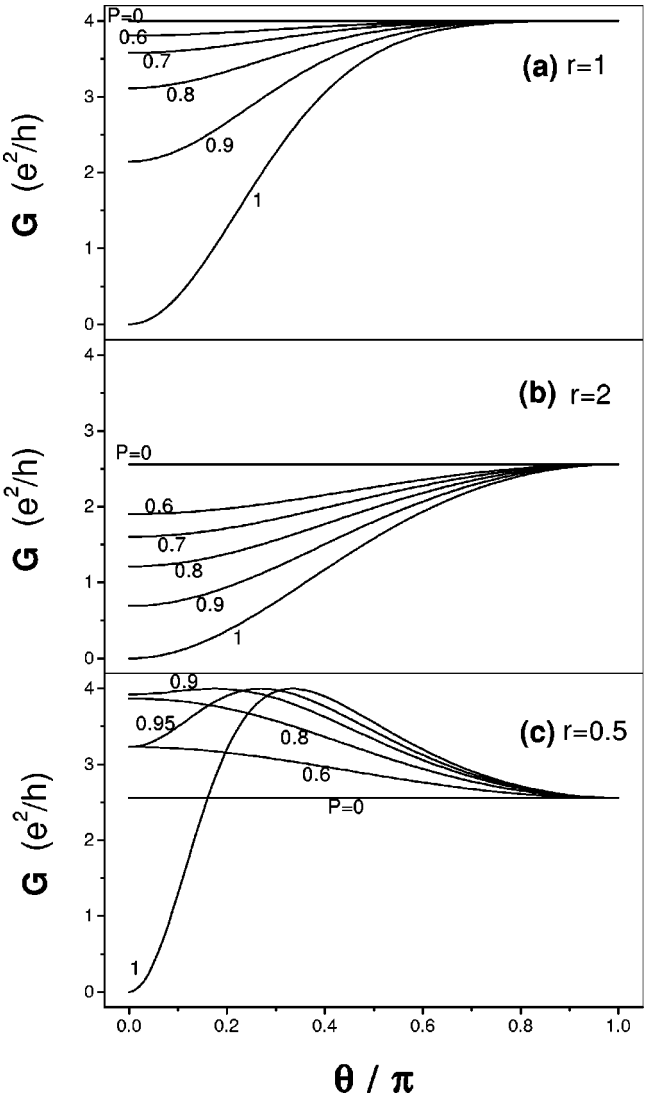

FIG. 3. The total conductance G vs θ for (F_1,F_2)-QD-S, where θ is the angle between the orientations of F_1 and F_2, with $\Gamma_1=\Gamma_2\equiv\Gamma$, $P_1=P_2\equiv P$, and $r\equiv\Gamma_0/(\Gamma_1+\Gamma_2)$.

where $r \equiv \Gamma_R/\Gamma_L$ is the ratio of the two coupling strengths. Analogous to the matching condition of the Fermi velocities in F/S contact (i.e., $k_{F\uparrow}k_{F\downarrow}=k_S^2$), here $P^2+r^2=1$ (i.e., $\Gamma_{L\uparrow}\Gamma_{L_\downarrow}=\Gamma_R^2$) plays the similar role. For $r>1$, the matching condition can never be satisfied, so G_{FDS} decreases monotonously with the increase of P [Fig. 2(a)]. While for $r<1$, there exists a certain value of P, say P_0, satisfying $P_0^2+r^2=1$, so G_{FDS} first increases with P , reaches its maximum value $4e^2/h$ at $P=P_0$, then drops to 0 when P approaches 1 [Fig. 2(b)]. This result warns us to be careful to deduce the spin polarization of F from AR conductance of F-QD-S.

Next, consider the general case of the three-terminal system (F_1,F_2)-QD-S. Similar to the composition of polarized light, the total current (or total conductance) of F_1 and F_2 are equivalent to that of an effective ferromagnet $\tilde{F}$. Introduce the spin-polarization vectors $\vec{q}_1$ and $\vec{q}_2$, where $\vec{q}_\beta$ has the magnitude of $\Gamma_\beta P_\beta$ and the direction of the magnetization direction of F_β, with β=1,2. It is easy to test that these vectors obey the vector composition rule, i.e., $\vec{q}=\vec{q}_1+\vec{q}_2$, in which $\vec{q}$ is the spin polarization vector of $\tilde{F}$. Therefore the effective parameters of $\tilde{F}$ are

$$\tilde{\Gamma}=\Gamma_1+\Gamma_2,$$

$$\tilde{P}=\frac{[(\Gamma_1P_1)^2+(\Gamma_2P_2)^2+2\Gamma_1P_1\Gamma_2P_2\cos\theta]^{1/2}}{\Gamma_1+\Gamma_2}. \quad (9)$$

As a result, the total conductance of F_1 and F_2 can be obtained as

$$G \equiv G_1+G_2=G_{FDS}(\tilde{P},\tilde{r}), \quad (10)$$

in which G_{FDS} has the same form as in Eq. (8), $\tilde{P}$ is the effective polarization, and $\tilde{r}$ is defined by $\Gamma_s/\tilde{\Gamma}$. Then the conductance of F_1 and F_2 can be expressed by the total conductance multiplied by a sharing factor,

$$G_1=G\frac{\Gamma_1^2+\Gamma_1\Gamma_2-(\Gamma_1^2P_1^2+\Gamma_1P_1\Gamma_2P_2\cos\theta)}{\Gamma_1^2+\Gamma_2^2+2\Gamma_1\Gamma_2-(\Gamma_1^2P_1^2+\Gamma_2^2P_2^2+2\Gamma_1P_1\Gamma_2P_2\cos\theta)}, \quad (11)$$

$$G_2=G\frac{\Gamma_2^2+\Gamma_1\Gamma_2-(\Gamma_2^2P_2^2+\Gamma_1P_1\Gamma_2P_2\cos\theta)}{\Gamma_1^2+\Gamma_2^2+2\Gamma_1\Gamma_2-(\Gamma_1^2P_1^2+\Gamma_2^2P_2^2+2\Gamma_1P_1\Gamma_2P_2\cos\theta)}. \quad (12)$$

Figure 3 shows the curves of G vs θ (which also can be viewed as $2G_1$ vs θ or $2G_2$ vs θ) for the symmetric case, in which $\Gamma_1=\Gamma_2\equiv\Gamma$ and $P_1=P_2\equiv P$. For $r=1$, G increases with the increase of θ or decrease of P. For $r>1$, the curves of G vs θ is qualitatively the same as those of $r=1$, but the conductance is lowered and more sensitive to P. For $r<1$, the variation is more complicated: if $P^2<1-r^2$, G decreases with the increase of θ or decrease of P; if $P^2>1-r^2$, G has the maximum $4e^2/h$ at θ satisfying $[P\cos(\theta/2)]^2=1-r^2$.

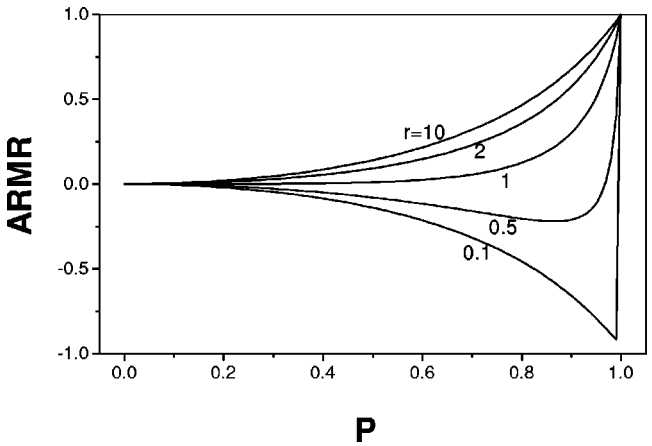

FIG. 4. ARMR vs P in (F_1,F_2)-QD-S, where ARMR$\equiv(G_{AF}-G_F)/(G_{AF}+G_F)$, P and r have the same meaning as in Fig. 3.

These results are readily understood by the new matching condition $\tilde{P}^2+r^2=1$ with the effective spin polarization $\tilde{P}=P\cos(\theta/2)$.

Two points are noteworthy in the above result: (i) If F_1 and F_2 are regarded as a whole, the effective polarization can be tuned continuously by changing the angle of the mutual orientations, which is impossible for one chosen ferromagnet. (ii) For $r\geqslant 1$, the total conductance for the two ferromagnets in antiferromagnetic alignment is larger than that in ferromagnetic alignment, which is completely different from the effect of GMR or TMR. To describe this interesting effect of magnetoresistance, define the ratio of Andreev reflected magnetic resistance (ARMR) in (F_1,F_2)-QD-S by

$$\text{ARMR} \equiv \frac{G_{AF}-G_F}{G_{AF}+G_F}. \quad (13)$$

the curves of ARMR vs P for various r are shown in Fig. 4.

Figure 5 shows the curves of G_1 vs θ for an asymmetric case, in which $P_1=1$, P_2 is arbitrary, and $\Gamma_1=\Gamma_2=\Gamma_s/2$. Since F_1 is fully polarized, the conductance of F_1 is sensitive to the spin polarization and orientation of F_2. For $P_2=0$, G_1 does not depend on θ; while for $P_2=1$, G_1 strongly depends on θ, with $G_1=0$ at $\theta=0$ and $G_1=4e^2/h$ at $\theta=\pi$. We suggest that this effect can be applied to measure the spin polarization of F_2. In practice, one may choose a half metal material as F_1, the ferromagnetic material to be measured as

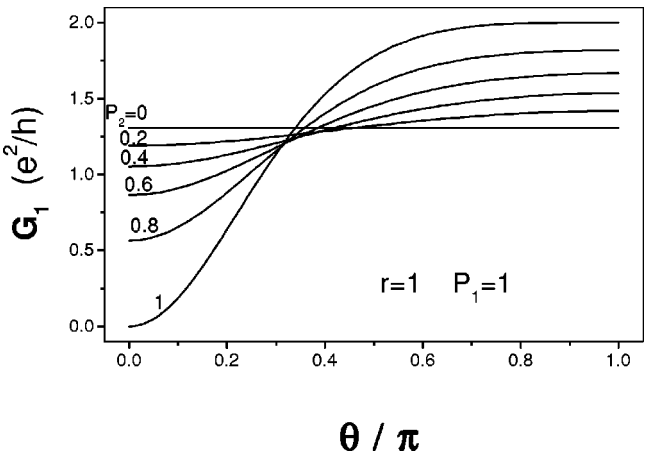

FIG. 5. The conductance G_1 vs θ for different P_2, with $P_1=1$ and $r=1$. G_1 has strong/weak dependence on θ for large/small P_2, which can be applied to measure the spin polarization of F_2.

F_2, and changing the spin orientation of F_1 by applying an external magnetic field, then the spin polarization of F_2 can be deduced from the weak/strong dependence of G_1 on θ.

IV. FINITE BIAS CURRENT

Now we turn to investigate the nonequilibrium transport of (F_1,F_2)-QD-S. For simplicity, we only consider the antiparallel orientation of F_1 and F_2 (i.e., $\theta=\pi$), with finite but small bias voltages (i.e., $|eV_1|<\Delta$ and $|eV_2|<\Delta$). Notice that the self-energy becomes block diagonal due to $\theta=\pi$, and the expression of current I_1 can be simplified as

$$I_1=\frac{e}{h}\int d\omega[A_{11}(f_1-\overline{f}_1)+A_{12}(f_1-\overline{f}_2)+Q_{1s}(f_1-f_s)+Q_{12}(f_1-f_2)], \tag{14}$$

$$A_{11}=\Gamma_{1\downarrow}\Gamma_{1\uparrow}|G^r_{12}|^2+\Gamma_{1\uparrow}\Gamma_{1\downarrow}|G^r_{34}|^2,$$

$$A_{12}=\Gamma_{2\uparrow}\Gamma_{1\uparrow}|G^r_{12}|^2+\Gamma_{2\downarrow}\Gamma_{1\downarrow}|G^r_{34}|^2,$$

$$Q_{1s}=\Gamma_{1\uparrow}\Gamma_s\tilde{\rho}\left[|G^r_{11}|^2+|G^r_{12}|^2+2\,\mathrm{Re}\left(-\frac{\Delta}{\omega}G^r_{11}G^{r*}_{12}\right)\right]+\Gamma_{1\downarrow}\Gamma_s\tilde{\rho}\left[|G^r_{33}|^2+|G^r_{34}|^2+2\,\mathrm{Re}\left(+\frac{\Delta}{\omega}G^r_{33}G^{r*}_{34}\right)\right],$$

$$Q_{12}=\Gamma_{2\downarrow}\Gamma_{1\uparrow}|G^r_{11}|^2+\Gamma_{2\uparrow}\Gamma_{1\downarrow}|G^r_{33}|^2.$$

At zero temperature and in the low bias regime, the current of the Q_{1s} process vanishes. Further assuming that both F_1 and F_2 are fully polarized, both Q_{12} and A_{11} processes are also forbidden. Only the process of A_{12}, i.e., crossed AR's involving F_1, F_2 and S, contributes to the current. I_1 and I_2 are derived as

$$I\equiv I_1=I_2=\frac{e}{h}\int d\omega\Gamma_{2\uparrow}\Gamma_{1\uparrow}|G^r_{12}|^2(f_1-\overline{f}_2). \tag{15}$$

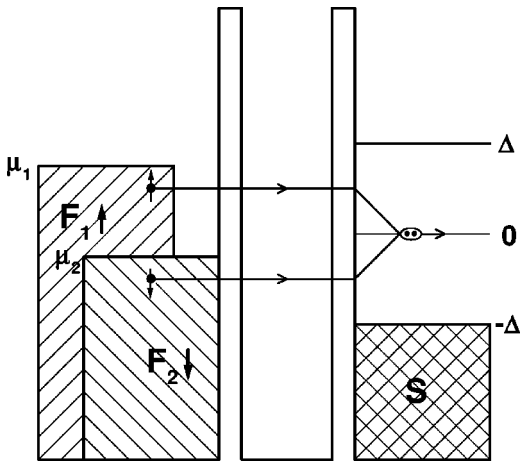

FIG. 6. Schematic diagram of nonequilibrium transport in (F_1,F_2)-QD-S. F_1 and F_2 are in antiferromagnetic alignment, marked by left- and right-slanted shadows, respectively. S is marked by crossed shadowing, with the energy gap region $\pm\Delta$ with respect to the chemical potential; QD is between the two barriers, and the energy structure is ignored for simplicity. The diagram illustrates an unusual property of the current conducted by crossed AR involving F_1, F_2, and S: the signs of I_1 or I_2 are determined by $\frac{1}{2}(\mu_1+\mu_2)$ rather than μ_1 or μ_2.

Notice that $I_1=I_2$ holds even if $\Gamma_1\neq\Gamma_2$ and $V_1\neq V_2$, because I_1 is pure spin↑ current and I_2 is pure spin↓ current while I_1+I_2 is required to be non-spin-polarized current by the superconductor. For simplicity, we further assume that $\Gamma_{1\uparrow}=\Gamma_{2\uparrow}\equiv\Gamma_L$ ($\Gamma_{1\downarrow}=\Gamma_{2\downarrow}=0$ due to $P_1=P_2=1$) and $\Gamma_s\equiv\Gamma_R$, then the system (F_1,F_2)-QD-S is similar to a special N-QD-S one, in which the two spin bands of N have different chemical potentials controlled by V_1 and V_2. Define the transmission probability of crossed AR's by $T_{AR}(\omega)\equiv\Gamma_L^2|G^r_{12}|^2$, the current can be expressed as

$$I=\frac{e}{h}\int_{-V_2}^{V_1}T_{AR}(\omega)d\omega. \tag{16}$$

Notice that $T_{AR}(\omega)$ is an even function of ω, the above current formula implies that the sign of I_1 or I_2 is not determined by V_1 or V_2 but by $\frac{1}{2}(V_1+V_2)$. This is quite unusual because it contains the case that $V_1>0$ and $V_2<0$ but $I_1=I_2>0$ (this unusual property was previously addressed in Ref. 20). Generally, for a three-terminal system, one may expect that current flows out of the terminal with highest voltage and into the terminal with lowest voltage. But for the current conducted by crossed AR's, the sign of current in each ferromagnetic terminal is linked to the averaged chemical potential of the two, because two ferromagnets cooperate with each other in this process, with total energy balanced. Figure 6 illustrates the conducting process corresponding to the case of $I_1=I_2>0$ with $\mu_1>0$ and $\mu_2<0$ but $\frac{1}{2}(\mu_1+\mu_2)>0$.

We ignore the energy structure of QD in Fig. 6 for simplicity, however, the current $I\equiv I_1=I_2$ depends strongly on the transmission probability of QD. In fact, I is the integral of $T_{AR}(\omega)$ over the range of $(-V_2,V_1)$. Figure 7 shows the

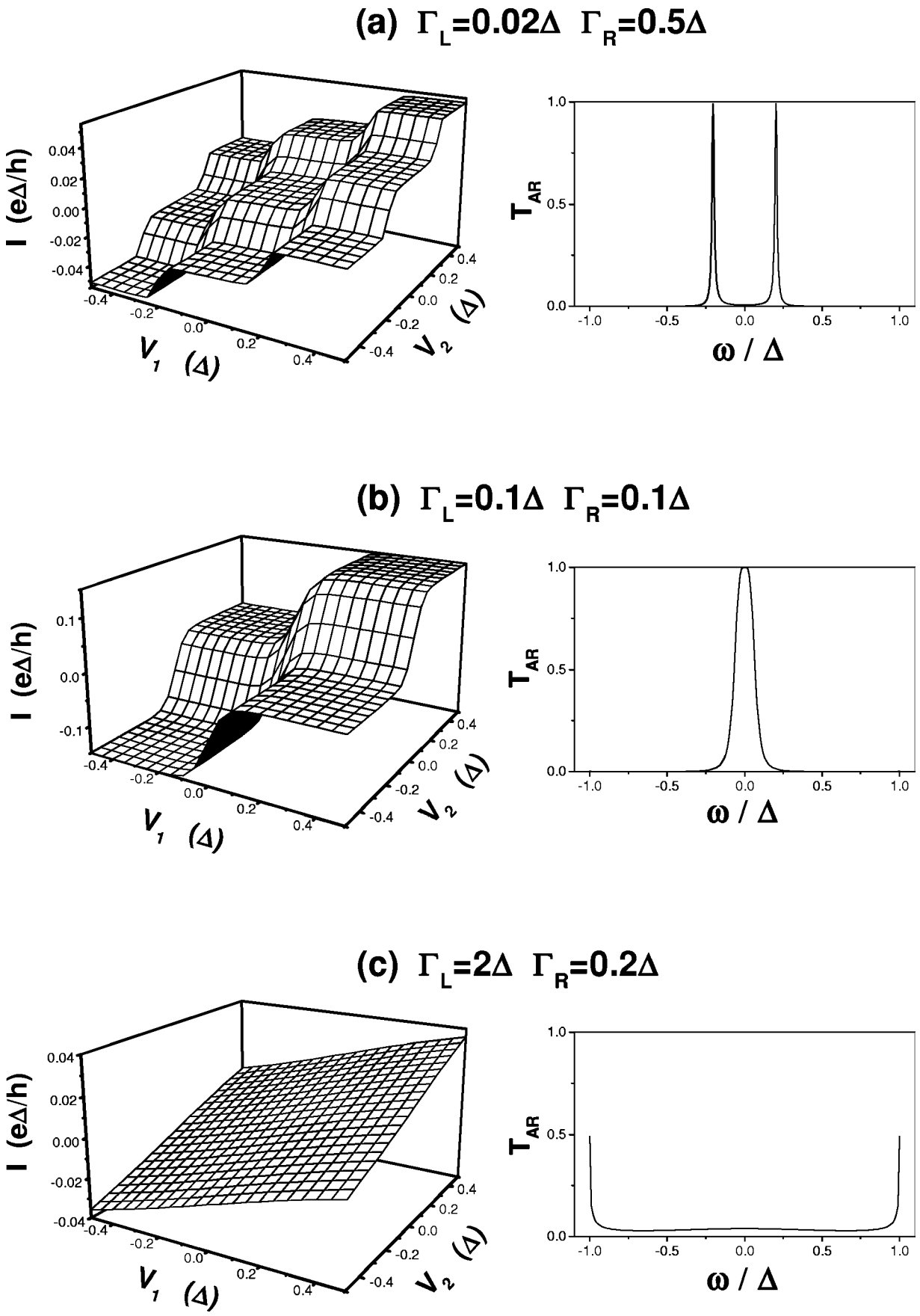

FIG. 7. The current $I \equiv I_1 = I_2$ vs the bias voltages (V_1, V_2) for three typical cases: (a) $\Gamma_L \ll \Gamma_R$; (b) $\Gamma_L = \Gamma_R$; and (c) $\Gamma_L \gg \Gamma_R$. The surface of $I(V_1, V_2)$ has a close relationship to the spectrum $T_{AR}(\omega)$, which can be used to extract the latter.

surfaces of $I(V_1,V_2)$ and corresponding $T_{AR}(\omega)$ spectrum for three typical cases of Γ_L and Γ_R. In Fig. 7(a), $\Gamma_L \ll \Gamma_R$, the spin degenerate level of QD is hybridized to two Andreev bound states due to coupling with S, while the coupling with F_1 and F_2 provides the small broadening to these bound states. T_{AR} has two peaks with the maximum of unity at each of the Andreev bound states. Correspondingly, the surface of $I(V_1,V_2)$ has five steps: the highest step corresponds to $(-V_2,V_1)$ covering both of the peaks; the second step (including two patches) corresponds to $(-V_2,V_1)$ covering one of the peaks; the third step (including three patches) corresponds to $(-V_2,V_1)$ or $(V_1,-V_2)$ covering none of the peaks; the fourth step (including two patches) corresponds to $(V_1,-V_2)$ covering one of the peaks; and the lowest step corresponds to $(V_1,-V_2)$ covering both of the peaks. In Fig. 7(b), $\Gamma_L=\Gamma_R$, the Andreev bound states are sufficiently broadened so that the two peaks in T_{AR} merge into one. The one peak structure of T_{AR} spectrum corresponds to three step pattern in $I(V_1,V_2)$ surface. In Fig. 7(c), $\Gamma_L \gg \Gamma_R$, the resonant level of QD is significantly broadened, as a result, T_{AR} is small and flat with tails at $\omega=\pm\Delta$. The structureless T_{AR} spectrum corresponds to a plain in $I(V_1,V_2)$ surface, proportional to $\frac{1}{2}(V_1+V_2)$. In short, the T_{AR} spectrum can be extracted from the measurement of the $I(V_1,V_2)$ surface.

V. CONCLUSIONS

In this paper, we have investigated the Andreev reflection in a (F_1,F_2)-QD-S system. By using the nonequilibrium Green function, a general current formula is derived, allowing arbitrary spin polarizations, magnetization orientations, and bias voltages in F_1 and F_2. The formula is applied to several special cases, revealing some interesting properties of this system: (i) Analogous to the Fermi velocity mismatch in F/S contact, the zero-bias conductance in F-QD-S reaches its maximum $4e^2/h$ if the matching condition $\Gamma_{L\uparrow}\Gamma_{L\downarrow}=\Gamma_R^2$ is satisfied. (ii) For total current (conductance) of (F_1,F_2)-QD-S with $V_1=V_2$, the two ferromagnets F_1 and F_2 are equivalent to an effective ferromagnet $\tilde{F}$, and the effective polarization $\tilde{P}$ can be tuned by the angle between the spin orientations of F_1 and F_2. (iii) There is a different effect of magnetoresistance in (F_1,F_2)-QD-S (named ARMR), in which the conductance for F_1 and F_2 in antiferromagnetic alignment is larger than that in ferromagnetic alignment. Based on this effect, a possible way to measure the spin polarization of ferromagnetic material is proposed. (iv) The nonequilibrium transport of this system is quite unusual. Especially if F_1 and F_2 are fully but opposite polarized, the signs of the current through F_1 and F_2 is determined by $\frac{1}{2}(V_1+V_2)$ rather than V_1 or V_2. Furthermore, the surface of $I(V_1,V_2)$ depends strongly on the AR transmission probability, which can be applied to extract the latter. Finally, we believe that the suggested (F_1,F_2)-QD-S system is accessible with up-to-date nano technology, and we are eager to see relevant experiments on such an appealing system.

ACKNOWLEDGMENTS

This project was supported by NSFC under Grant No. 10074001. We would like to thank Y. Lu and Y. F. Yang for useful discussions. One of the authors (T.-H. Lin) would also like to acknowledge the support from the Visiting Scholar Foundation of State Key Laboratory for Mesoscopic Physics in Peking University.

APPENDIX

In this Appendix, we present the detailed derivation of the formulas (3)–(7) by using the nonequilibrium Green function and introducing a 4×4 matrix representation.

Since the current through QD can be expressed in terms of the Green functions of QD, we first derive the retarded and distribution Green functions by the Dyson equation and the Keldysh equation. To include the physics of Andreev reflections and the spin-flip processes in a unified formulation, we introduce a 4×4 matrix representation, in which the Green function is defined as

$$\mathbf{G}\equiv\left\langle\left\langle \begin{pmatrix} c_\uparrow \\ c_\downarrow^\dagger \\ c_\downarrow \\ c_\uparrow^\dagger \end{pmatrix} \middle| (c_\uparrow^\dagger \;\; c_\downarrow \;\; c_\downarrow^\dagger \;\; c_\uparrow) \right\rangle\right\rangle. \tag{A1}$$

The physical meaning of the elements of **G** is illustrated in the following:

$e\uparrow\longleftarrow e\uparrow$	$e\uparrow\longleftarrow h\uparrow$	$e\uparrow\longleftarrow e\downarrow$	$e\uparrow\longleftarrow h\downarrow$
$h\uparrow\longleftarrow e\uparrow$	$h\uparrow\longleftarrow h\uparrow$	$h\uparrow\longleftarrow e\downarrow$	$h\uparrow\longleftarrow h\downarrow$
$e\downarrow\longleftarrow e\uparrow$	$e\downarrow\longleftarrow h\uparrow$	$e\downarrow\longleftarrow e\downarrow$	$e\downarrow\longleftarrow h\downarrow$
$h\downarrow\longleftarrow e\uparrow$	$h\downarrow\longleftarrow h\uparrow$	$h\downarrow\longleftarrow e\downarrow$	$h\downarrow\longleftarrow h\downarrow$

(A2)

in which $e\uparrow\leftarrow h\downarrow$ represents the process that a hole with spin$\downarrow$ is converted into an electron with spin$\uparrow$, etc.

Let $\mathbf{G}^r$ denote the Fourier transformed retarded Green function of QD, and $\mathbf{G}^r$ can be solved by the Dyson equation

$$\mathbf{G}^r=\mathbf{g}^r+\mathbf{g}^r\mathbf{\Sigma}^r\mathbf{G}^r, \tag{A3}$$

in which $\mathbf{g}^r$ is the retarded Green function of an isolated QD and $\mathbf{\Sigma}^r$ is the self-energy due to couplings between QD and leads. $\mathbf{g}^r$ can be easily obtained as

$$\mathbf{g}^r=\begin{pmatrix} \dfrac{1}{\omega-E_0+\mathrm{i}0^+} & 0 & 0 & 0 \\ 0 & \dfrac{1}{\omega+E_0+\mathrm{i}0^+} & 0 & 0 \\ 0 & 0 & \dfrac{1}{\omega-E_0+\mathrm{i}0^+} & 0 \\ 0 & 0 & 0 & \dfrac{1}{\omega+E_0+\mathrm{i}0^+} \end{pmatrix}, \tag{A4}$$

while $\mathbf{\Sigma}^r$ consists of three parts,

$$\mathbf{\Sigma}^r=\mathbf{\Sigma}_1^r+\mathbf{\Sigma}_2^r+\mathbf{\Sigma}_s^r. \tag{A5}$$

$\mathbf{\Sigma}_1^r$ is the self-energy from the coupling between QD and F_1, given by

$$\mathbf{\Sigma}_1^r=-\frac{\mathrm{i}}{2}\begin{pmatrix} \Gamma_{1\uparrow} & 0 & 0 & 0 \\ 0 & \Gamma_{1\downarrow} & 0 & 0 \\ 0 & 0 & \Gamma_{1\downarrow} & 0 \\ 0 & 0 & 0 & \Gamma_{1\uparrow} \end{pmatrix}, \tag{A6}$$

in which $\Gamma_{1\uparrow}$ and $\Gamma_{1\downarrow}$ are the spin-dependent coupling strengths defined by $\Gamma_{1\sigma}\equiv 2\pi N_{1\sigma}|t_{1\sigma}|^2$, with $N_{1\sigma}$ being the density of states of spin σ band of F_1. $\mathbf{\Sigma}_2^r$ is the self-energy from the coupling between QD and F_2, given by

$$\mathbf{\Sigma}_2^r=-\frac{\mathrm{i}}{2}\begin{pmatrix} c^2\Gamma_{2\uparrow}+s^2\Gamma_{2\downarrow} & 0 & sc(\Gamma_{2\uparrow}-\Gamma_{2\downarrow}) & 0 \\ 0 & c^2\Gamma_{2\downarrow}+s^2\Gamma_{2\uparrow} & 0 & sc(\Gamma_{2\uparrow}-\Gamma_{2\downarrow}) \\ sc(\Gamma_{2\uparrow}-\Gamma_{2\downarrow}) & 0 & c^2\Gamma_{2\downarrow}+s^2\Gamma_{2\uparrow} & 0 \\ 0 & sc(\Gamma_{2\uparrow}-\Gamma_{2\downarrow}) & 0 & c^2\Gamma_{2\uparrow}+s^2\Gamma_{2\downarrow} \end{pmatrix}, \tag{A7}$$

in which $s\equiv\sin(\theta/2)$, $c\equiv\cos(\theta/2)$, $\Gamma_{2\uparrow}$, and $\Gamma_{2\downarrow}$ are defined similarly to $\Gamma_{1\uparrow}$ and $\Gamma_{1\downarrow}$. $\mathbf{\Sigma}_s^r$ is the self-energy from the coupling between QD and *S*, given by

$$\mathbf{\Sigma}_s^r=-\frac{\mathrm{i}}{2}\Gamma_s\rho(\omega)\begin{pmatrix} 1 & -\dfrac{\Delta}{\omega} & 0 & 0 \\ -\dfrac{\Delta}{\omega} & 1 & 0 & 0 \\ 0 & 0 & 1 & \dfrac{\Delta}{\omega} \\ 0 & 0 & \dfrac{\Delta}{\omega} & 1 \end{pmatrix}, \tag{A8}$$

in which $\Gamma_s\equiv 2\pi N_s|t_s|^2$, with N_s being the density of states when the superconductor is in the normal state, $\rho(\omega)$ is the modified BCS density of states defined by

$$\rho(\omega)\equiv\begin{cases} \dfrac{|\omega|}{\sqrt{\omega^2-\Delta^2}} & |\omega|>\Delta \\ \dfrac{\omega}{\mathrm{i}\sqrt{\Delta^2-\omega^2}} & |\omega|<\Delta. \end{cases} \tag{A9}$$

Thus $\mathbf{G}^r$ can be obtained by solving the Dyson equation, Eq. (A3).

Let $\mathbf{G}^<$ denote the Fourier transformed distribution Green function of QD, and $\mathbf{G}^<$ can be obtained by the Keldysh equation

$$\mathbf{G}^<=\mathbf{G}^r\mathbf{\Sigma}^<\mathbf{G}^a. \tag{A10}$$

Notice that the advanced Green function and self-energy are the Hermitian conjugations of the corresponding retarded Green function and self-energy. And $\mathbf{\Sigma}^<$ can be obtained by applying the fluctuation-dissipation theorem to each of $\mathbf{\Sigma}_1^<$, $\mathbf{\Sigma}_2^<$, and $\mathbf{\Sigma}_s^<$,

$$\begin{aligned} \mathbf{\Sigma}^<&=\mathbf{\Sigma}_1^<+\mathbf{\Sigma}_2^<+\mathbf{\Sigma}_s^<, \\ \mathbf{\Sigma}_1^<&=\mathbf{F}_1(\mathbf{\Sigma}_1^a-\mathbf{\Sigma}_1^r), \\ \mathbf{\Sigma}_2^<&=\mathbf{F}_2(\mathbf{\Sigma}_2^a-\mathbf{\Sigma}_2^r), \\ \mathbf{\Sigma}_s^<&=\mathbf{F}_s(\mathbf{\Sigma}_s^a-\mathbf{\Sigma}_s^r), \end{aligned} \tag{A11}$$

in which

$$\mathbf{F}_1=\begin{pmatrix} f_1 & 0 & 0 & 0 \\ 0 & \overline{f_1} & 0 & 0 \\ 0 & 0 & f_1 & 0 \\ 0 & 0 & 0 & \overline{f_1} \end{pmatrix}, \tag{A12}$$

$$\mathbf{F}_2=\begin{pmatrix} f_2 & 0 & 0 & 0 \\ 0 & \overline{f_2} & 0 & 0 \\ 0 & 0 & f_2 & 0 \\ 0 & 0 & 0 & \overline{f_2} \end{pmatrix}, \tag{A13}$$

$$\mathbf{F}_s=\begin{pmatrix} f & 0 & 0 & 0 \\ 0 & f & 0 & 0 \\ 0 & 0 & f & 0 \\ 0 & 0 & 0 & f \end{pmatrix}, \tag{A14}$$

where f_1, $\overline{f_1}$, f_2, $\overline{f_2}$, and f denote $f(\omega-V_1)$, $f(\omega+V_1)$, $f(\omega-V_2)$, $f(\omega+V_2)$, and $f(\omega)$, respectively, in which $f(\omega)$ is the Fermi distribution function.

Then, the current flowing from F_1 to the QD can be expressed in terms of $\mathbf{G}^r$ and $\mathbf{G}^<$ as

$$I_1=I_{1\uparrow}+I_{1\downarrow}=\frac{e}{h}\int d\omega[(\mathbf{G}\Sigma_1)^<+\text{H.c.}]_{11+33}, \tag{A15}$$

in which we have used the compact notations $[\mathbf{AB}]^< \equiv \mathbf{A}^r\mathbf{B}^< + \mathbf{A}^<\mathbf{B}^a$ and $[\ ]_{11+33}\equiv[\ ]_{11}+[\ ]_{33}$. After some algebraic manipulations, the current can be divided into contributions from four conducting processes, as shown and interpreted in Sec. II.

*Author to whom correspondence should be addressed.

[1] G.A. Prinz, Prog. Photovoltaics **48**(4), 58 (1995).
[2] C.J. Lambert and R. Raimondi, J. Phys.: Condens. Matter **10**, 901 (1998).
[3] G.E. Blonder, M. Tinkham, and T.M. Klapwijk, Phys. Rev. B **25**, 4515 (1982).
[4] M.J.M. de Jong and C.W. Beenakker, Phys. Rev. Lett. **74**, 1657 (1995).
[5] S.K. Upadhyay, A. Palanisami, R.N. Louie, and R.A. Buhrman, Phys. Rev. Lett. **81**, 3247 (1998).
[6] R.J. Soulen, Jr., J.M. Byers, M.S. Osofsky, N. Nadgorny, T. Ambrose, T. Ambrose, S.F. Cheng, P.R. Broussard, C.T. Tanaka, J. Nowak, J.S. Moodera, A. Barry, and J.M.D. Coey, Science **282**, 85 (1998).
[7] I. Žutić and O.T. Valls, Phys. Rev. B **60**, 6320 (1999); **61**, 1555 (2000).
[8] S. Kashiwaya, Y. Tanakan, N. Yoshida, and M.R. Beasley, Phys. Rev. B **60**, 3572 (1999).
[9] M. Giroud, H. Courtois, K. Hasselbach, D. Mailly, and B. Pannetier, Phys. Rev. B **58**, R11 872 (1998).
[10] V.T. Petrashov, I.A. Sosnin, I. Cox, A. Parsons, and C. Troadec, Phys. Rev. Lett. **83**, 3281 (1999).
[11] S. Takahashi, H. Imamura, and S. Maekawa, Phys. Rev. Lett. **82**, 3911 (1999).
[12] L.R. Tagirov, Phys. Rev. Lett. **83**, 2058 (1999).
[13] M.L. Kulić and M. Endres, Phys. Rev. B **62**, R11 846 (2000).
[14] S.-K. Yip, Phys. Rev. B **62**, R6127 (2000).
[15] T.T. Heikkilä, F.K. Wilhelm, and G. Schön, Europhys. Lett. **51**, 434 (2000).
[16] A. Kadigrobov, R.I. Shekhter, M. Jonson, and Z.G. Ivanov, Phys. Rev. B **60**, 14 593 (1999).
[17] V. Prokić, A.I. Buzdin, and L. Dobrosavljević-Grujić, Phys. Rev. B **59**, 587 (1999).
[18] F. Taddei, S. Sanvito, J.H. Jefferson, and C.J. Lambert, Phys. Rev. Lett. **82**, 4938 (1999).
[19] F. Taddei, S. Sanvito, and C.J. Lambert, cond-mat/0003345 (unpublished).
[20] G. Deutscher and D. Feinberg, Appl. Phys. Lett. **76**, 487 (2000).
[21] J.C. Cuevas, A. Marín-Rodero, and A.L. Yeyati, Phys. Rev. B **54**, 7366 (1996).
[22] Q.-F. Sun, J. Wang, and T.-H. Lin, Phys. Rev. B **59**, 3831 (1999).